Supporting Information

Yu et al. 10.1073/pnas.1008296107

SI Text

Reproducing the Standard Conventional Limit for Cells with Nonisotropic Response. This section expands upon the discussion on light trapping in bulk structures, by considering the case where the resonances do not couple to channels isotropically. Suppose the resonances in the structure only couple to light with incident angle less than θ. In applying Eq. **6** to calculate the upper limit for the absorption enhancement factor, we only need to include channels with a radius of $k_{//} = \sin(\theta)\omega/c$ in the $k_{//}$ space:

$$N = \frac{2\pi \sin^2(\theta)\omega^2}{c^2}\left(\frac{L}{2\pi}\right)^2. \qquad [S1]$$

Therefore, the upper limit for the absorption enhancement factor is

$$F = \frac{4n^2}{\sin^2(\theta)}. \qquad [S2]$$

This result agrees with that of ray-optics theory (1, 2).

Analytic Calculation of the Light-Trapping Limit of the Simulated Structure. In this section, we use our theory to calculate the upper limit of the absorption enhancement factor for the structure shown in Fig. 3*A*. The structure in Fig. 3*A* consists of four layers, a top scattering layer, a cladding layer, an active layer, and a mirror plate. In order to determine the upper limit for the absorption enhancement factor, the first step is to calculate the guided mode profiles. For this calculation, we approximate the scattering layer as a uniform layer with its refractive index ($n^2 = 4.64$) determined by averaging the dielectric and air regions. The whole structure supports three waveguide modes at 500 nm wavelength. For each waveguide mode, its loss α_{wg} and group index n_{wg} are calculated directly by mode solving. Its contribution to the upper limit of absorption enhancement factor is then calculated as

$$F = \frac{\alpha_{wg}}{\alpha_0}\frac{\lambda}{d}n_{wg}, \qquad [S3]$$

where the absorption coefficient of the material in the active layer is $\alpha_0 = 400\ \mathrm{cm}^{-1}$, and the thickness of the active layer is $d = 5$ nm. The computations for these modes are summarized in Table S1. It is known that only transverse magnetic (TM) modes have the slot-waveguide effect with the field strongly enhanced in the low-index active layers (3). Here we indeed see significant contributions to the absorption enhancement only from TM modes (Fig. S1). The predicted upper limit, summing over the contributions of all three modes, is 147.

Details of the Simulated Structure. In this section, we provide detailed information about the simulations performed to obtain the absorption spectra for the structures shown in Fig. 3*A*. A scattering-matrix-based numerical simulation was used; details can be found in ref. 4. This method first solves the electromagnetic field in the spatial Fourier space for each layer, and then determines the scattering matrix of the overall structure by matching the boundary conditions between different layers. The number of spatial Fourier components used is 21×21.

The scattering layer has a square lattice with a period $L = 1{,}200$ nm and a thickness of 80 nm. Each unit cell consists of a number of air grooves cutting through the high-dielectric material ($n^2 = 12.5$). There are three sets of air grooves. The first set consists of 10 grooves with width $0.05L$, aligned along the axial direction through the center of the unit cell. These grooves are evenly distributed every 18 deg starting from the [10] direction. The second set consists of two grooves with $0.1L$ width oriented along [11] and [−11] directions. Lastly, two concentric rings ($0.05L$ in width) with radius $0.25L$ and $0.48L$ are introduced to further increase the scattering strength. The scattering layer is then discretized by a 50×50 grid mesh (Fig. S2). Using this mesh, the Fourier components (4) of the dielectric function are calculated by

$$F_{kx,ky} = \frac{1}{2500}\sum_{i,j=1,\ldots,50}\varepsilon(x_i,y_j)e^{-i(k_x x_i + k_y y_j)}.$$

We note that there is in fact no stringent requirement on the design of the scattering pattern, e.g., a wide range of widths and number of air grooves can be used.

Detailed Derivation of Some of the Main Equations in Paper. ***Eq. 2 of the main text: Single resonance absorption spectrum A(ω).*** The amplitudes of resonance and incident channel can be written as

$$a(t) = a(\omega)\exp(j\omega t) \qquad S(t) = S(\omega)\exp(j\omega t), \qquad [S4]$$

where $a(\omega)$ and $S(\omega)$ are spectra of the resonance and incident channel. Substituting into Eq. **1** of the main text, we obtain the spectrum of the resonance amplitude

$$a(\omega) = \frac{j\sqrt{\gamma_e}S(\omega)}{(j(\omega-\omega_0) + (\gamma_i + N\gamma_e)/2}. \qquad [S5]$$

The absorption spectrum can be calculated as

$$A(\omega) = \frac{\gamma_i|a(\omega)|}{|S(\omega)|} = \frac{\gamma_i\gamma_e}{(\omega-\omega_0)^2 + (\gamma_i + N\gamma_e)^2/4}. \qquad [S6]$$

Eq. 7 of the main text: Number of resonant modes M. We consider the photon density of states in a medium that has a thickness d, and a square lattice with a periodicity L. In k space, each resonant mode occupies a volume of $\Delta V_k = \frac{2\pi}{d}\times\frac{2\pi}{L}\times\frac{2\pi}{L}$. The total number of resonances below frequency ω is obtained by counting resonant modes within the sphere specified by radius $k_0 = n\omega/c$:

$$m = 2\times\frac{4\pi}{3}k_0^3\times\frac{1}{\Delta V_k} = \frac{8\pi}{3}\frac{n^3\omega^3}{c^3}\left(\frac{L}{2\pi}\right)^2\frac{d}{2\pi}, \qquad [S7]$$

where the factor of 2 arises from the two polarizations of light. The number of resonances in the frequency range $[\omega,\omega+\delta\omega]$ is then

$$M = \frac{8\pi n^3\omega^2}{c^3}\left(\frac{L}{2\pi}\right)^2\frac{d}{2\pi}\delta\omega. \qquad [S8]$$

Eq. 8 of the main text: Number of channels N. The number of channels is counted in two-dimensional $k_{//}$ space (Fig. 2*A* of the main text). With a period L, each channel takes an area $\frac{2\pi}{L}\times\frac{2\pi}{L}$. All

channels have parallel wavevectors that satisfy $k_{//} < k_0 = \omega/c$. Thus

$$N = 2 \times \pi k_0^2 \times \frac{1}{(2\pi/L)^2} = \frac{2\pi\omega^2}{c^2}\left(\frac{L}{2\pi}\right)^2. \quad \text{[S9]}$$

Again, a factor of 2 arises from two polarizations.

Eq. 10 of the main text: Number of resonances formed by a single waveguide mode. In contrast to Eq. **7**, here the number of resonances is counted in k_{xy} space because there is only one mode in the z direction. The area that each resonance occupies in k_{xy} space is $\frac{2\pi}{L} \times \frac{2\pi}{L}$. The number of resonances below frequency ω is counted within the circle of radius $k_0 = n_{wg}\omega/c$:

$$m = 2 \times \pi k_0^2 \times \frac{1}{(2\pi/L)^2} = 2 \times \frac{\pi n_{wg}^2 \omega^2}{c^2}\left(\frac{L}{2\pi}\right)^2, \quad \text{[S10]}$$

where n_{wg} is the group index of the single mode. For convenience, we assume n_{wg} does not change with frequency and polarization. In the frequency range $[\omega,\omega + \delta\omega]$,

$$M = 2 \times \frac{2\pi {n_{wg}}^2 \omega}{c^2}\left(\frac{L}{2\pi}\right)^2 \delta\omega. \quad \text{[S11]}$$

Absorption Enhancement Without a Perfect Electric Conductor (PEC) Mirror. A PEC mirror is not essential to obtain high light-trapping-based absorption enhancement. Here we consider a structure similar to Fig. 3*A*, except that the PEC mirror is replaced by a dielectric layer with a thickness of 60 nm and a dielectric constant of $n_H = \sqrt{12.5}$ (Fig. S3*A*). The averaged enhancement factor in this case becomes 67 (Fig. S3*B*), which is still well above $4n^2 = 10$. This enhancement factor is about half of the enhancement factor shown in Fig. 4*A* of main text due to the lack of a reflecting mirror.

1. Campbell P, Green MA (1987) Light trapping properties of pyramidally textured surfaces. *J Appl Phys* 62:243–249.
2. Yablonovitch E (1982) Statistical ray optics. *J Opt Soc Am A* 72:899–907.
3. Almeida VR, Xu Q, Barrios CA, Lipson M (2004) Guiding and confining light in void nanostructure. *Opt Lett* 29:1209–1211.
4. Tikhodeev SG, Yablonskii AL, Muljarov EA, Gippius NA, Ishihara T (2002) Quasiguided modes and optical properties of photonic crystal slabs. *Phys Rev B* 66:045102.

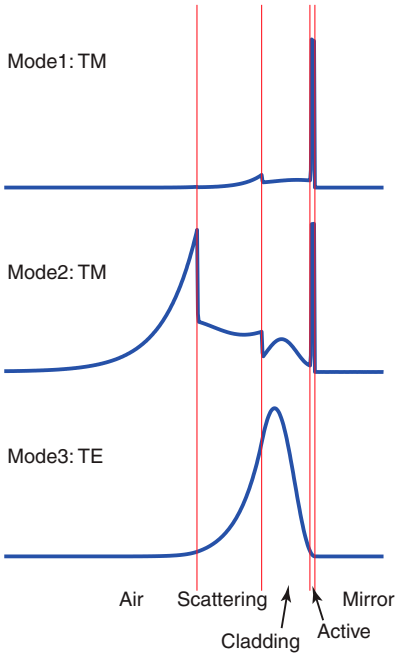

Fig. S1. Profiles of electric-field intensity for the waveguide modes.

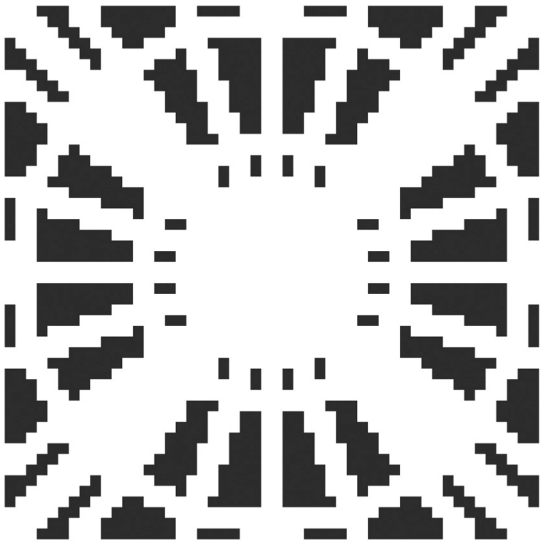

Fig. S2. The real-space pattern of the scattering layer. Black corresponds to high-dielectric regions. White regions are air.

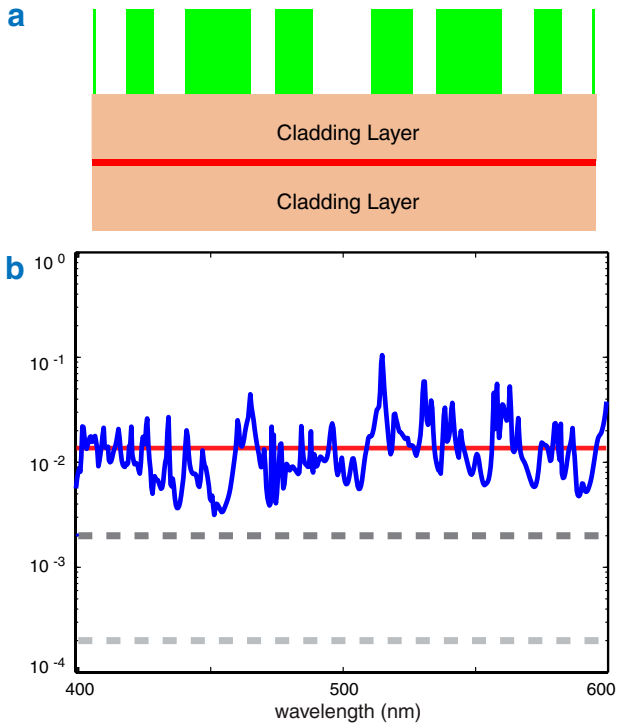

Fig. S3. (*A*) Light-trapping structure where PEC is replaced by a cladding layer. (*B*) Absorption spectrum for the structure shown in *A*.

Table S1. Absorption coefficients and enhancement factor of waveguide modes

Mode	Mode1 TM	Mode2 TM	Mode3 TE
α_{wg}/α_0	0.37	0.069	0.00053
n_{wg}	3.4	3.2	3.9
λ/d ($\lambda = 500$ nm)	100	100	100
Enhancement	125	22	0.2
Total enhancement limit	147.2		

TM, transverse magnetic; TE, transverse electric.